

Gaussian-Mixture Modelling of A-Mode Radiofrequency Scans for the Measurement of Arterial Wall Thickness

Raj Kiran V, Nabeel P M, *Member, IEEE*, Malay Ilesh Shah, Mohanasankar Sivaprakasam, and Jayaraj Joseph

Abstract— Measurement of arterial wall thickness is an integral component of vascular properties and health assessment. State-of-the-art automated or semi-automated techniques are majorly applicable to B-mode images and are not available for entry-level in-expensive devices. Considering this, we have earlier developed and validated an image-free (A-mode) ultrasound device, ARTSENS® for the evaluation of vascular properties. In this work, we present a novel gaussian-mixture modeling-based method to measure arterial wall thickness from A-mode frames, which is readily deployable to the existing technology. The method's performance was assessed based on systematic simulations and controlled phantom experiments. Simulations revealed that the method could be confidently applied to A-mode frames with above-moderate SNR (>15 dB). When applied to A-mode frames acquired from the flow-phantom setup (SNR > 25 dB), the mean error was limited to ($2 \pm 1\%$), and RMSE was 19 μm , on comparison with B-mode measurements. The measured and reference wall thickness strongly agreed with each other ($r = 0.88$, insignificant mean bias = 7 μm , $p = 0.16$). The proposed method was capable of performing real-time measurements.

Clinical Relevance— While the wall thickness estimates provided by this image-free method are not a replacement to image-based measures, but would potentially serve several emerging alleys such as real-time assessment of material properties, low-cost devices, large population screening etcetera.

I. INTRODUCTION

Ultrasound-based measurement of arterial wall thickness is an established and widely measured sub-clinical parameter for cardiovascular (CV) risk management. With age, the structure and function of arteries deteriorate, the rate of which is dependent on several modifiable and non-modifiable risk factors such as lifestyle, environment, genetics, etc. Conventional blood markers are fluctuating in nature, not providing adequate information on the disease progression till late stages [1]. Therefore, early screening strategies based on evaluation of the structural and functional properties that manifest arterial stiffening have gained significant attention over the last decade. Measurement of arterial wall thickness, given as intima-media thickness (IMT), plays a critical role in this regard. This geometric measure is an established marker of the structural remodeling of the arterial walls and has been

Raj Kiran V and Jayaraj Joseph are with the Department of Electrical Engineering, Indian Institute of Technology Madras, Chennai, India (e-mail: ee15d020@ee.iitm.ac.in).

Nabeel PM and Malay Ilesh Shah are with Healthcare Technology Innovation Centre, Indian Institute of Technology Madras, Chennai, India.

Mohanasankar Sivaprakasam is with the Department of Electrical Engineering and the Director of Healthcare Technology Innovation Centre, Indian Institute of Technology Madras, Chennai, India.

used as a clinical end-point in numerous investigative studies quantifying the effect of atherosclerotic preventive measures [2], [3]. Further, evaluation of several clinically relevant functional properties such as local pulse wave velocity, modulus of elasticity, vessel wall stress, etc., are possible with the measurement of IMT [4]–[6].

Current methods apply to B-mode images obtained by an imaging ultrasound system and are often performed manually, which are prone to inherent higher inter/intra operator variabilities. Automated and semi-automated methods, reviewed in [7], on the other hand, provide more precise measurements, the reliability of which are seldom operator dependent. Such state-of-art techniques are not available in entry-level ultrasound devices and are considerably expensive for resource constraints settings. We have earlier developed an image-free ultrasound technology ARTSENS®, specifically to address the need for a convenient, inexpensive, portable, and field amenable device for automated assessment of vascular properties [8]–[10]. In this work, we have developed a novel method for image-free measurement of arterial wall thickness in terms of a surrogate intima-media thickness (sIMT), that can be installed to ARTSENS®. With the help of systematic simulations and a controlled in-vitro study, we have demonstrated the method's functionality.

II. MATERIALS AND METHODS

A. Guidelines for IMT measurement

Given the important role of non-invasive IMT measurement, researchers and clinicians acknowledged the need to standardize the measurement method [11]. Wikstrand [11], discusses few critical aspects of measuring the IMT, which are enlisted here. Adventitia and intima layers of arterial walls are echogenic, and media, on the contrary, is hypoechoic, resulting in a characteristic double line pattern for the arterial wall echoes in ultrasound images. The echoes' width doesn't provide any anatomical feature of the arterial wall layers; rather, their leading edges provide the anatomical locations of layers. Therefore, IMT should be measured from the leading edges of the characteristic double line echo patterns formed by the walls. Further, even if a double-line pattern is clearly visible for proximal wall echoes, it is recommended to perform measurements on the distal wall for valid IMT. This is because the leading edges of the distal wall's double-line pattern signify the anatomical locations of lumen-intima (LI) and media adventitia (MA) interfaces. In the presented work, the wall thickness is measured from the distal wall, where the leading edges of the distal wall's echo pair are estimated based on a gaussian mixture modeling approach. The proposed method uses one-

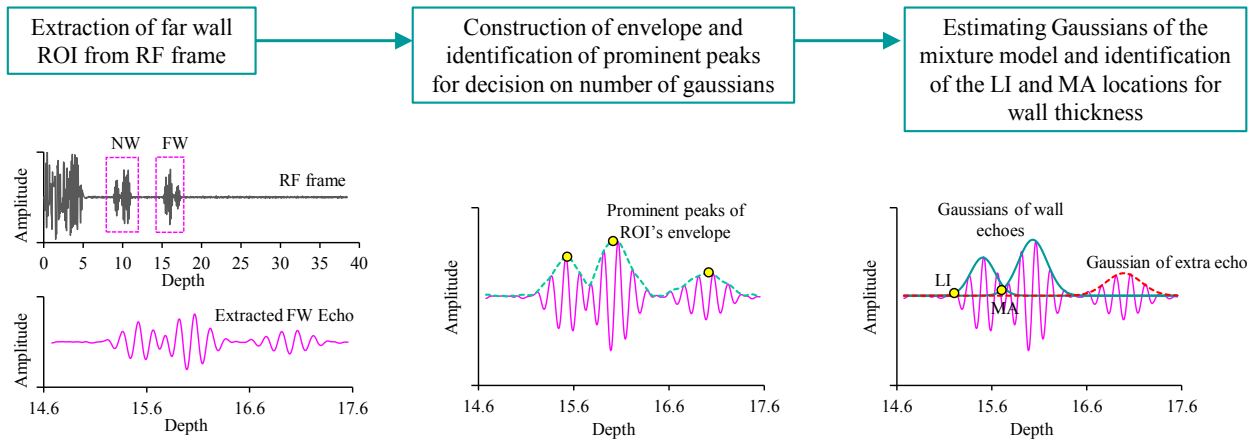


Figure 1. Illustration of various stages involved in the Gaussian mixture model method to estimate the wall thickness.

dimensional A-mode frames (image-free technique) for doing so, and therefore, the evaluated wall thickness is presented as surrogate IMT (sIMT).

B. Gaussian-mixture Modelling Approach

A-mode frames consist of raw RF echoes, and those can be approximately represented by a model as a sum of weighted and shifted Gaussian modulated sinusoidal pulses [12]. Each pulse originates at an anatomical location of a new tissue interface. Assuming there are ‘M’ such interfaces, the A-mode frame $r(n)$ can be expressed as

$$r(n) = \sum_{m=1}^M s_m(n) + w(n) \quad (1)$$

Where $w(n)$ is the white noise and $s_m(n)$ is the m^{th} weighted Gaussian modulated sinusoidal pulse,

$$s_m(n) = G_m \cos(2\pi f_c(n - \tau_m) + \theta_m). \quad (2)$$

Here, G_m represents the weighted gaussian that modulates m^{th} echo pulse, the amplitude of which depends on the echogenicity of the respective tissue structure, τ is the delay of the pulse as a result of scatterer-to-skin-surface distance, f_c is the center frequency of the ultrasound transducer, and θ_m is the phase offset of the m^{th} sinusoid pulse. Now, an envelop constructed on this A-mode frame, therefore, can be modeled by a mixture of ‘M’ Gaussians that modulate the sinusoidal pulses. From expression (2), G_m , i.e., any m^{th} gaussian is given as,

$$G_m(n) = A_m e^{-0.5 * \left(\frac{n-b_m}{c_m}\right)^2}, \quad (3)$$

where A_m is the amplitude, b_m is the location of the peak, and c_m is the standard deviation of the respective m^{th} gaussian.

C. Identification of LI and MA for estimation of sIMT

The method proposed here exploits this modeling approach to estimate the leading edges of the intima and adventitia echoes of the far wall, which correspond to LI and MA interfaces and thereby evaluates sIMT. An overall schematic of the method is shown in Fig. 1, taking a simple example for illustrative purpose. Since the sIMT measurements are performed on the distal wall, its real-time location in each recorded A-mode frame is to be identified, and a region of interest encompassing the wall echoes is to be

extracted first. For this, we have earlier developed and validated robust automated methods, the details of which can be found elsewhere [10]. The extracted distal wall ROI forms the input to the proposed method, and it consists of a series of gaussian modulated sinusoids. The peaks of the sinusoids were detected based on a second derivative-based peak-detector algorithm, and an envelop signal, $E(n)$, of the ROI, is constructed by applying cubic spline interpolation on these peaks. The ROI and its envelop constructed in this manner are equal in length.

Samples in $E(n)$ is now modeled by a function, in (4), that nonlinearly combines the model parameters $\{A_m\}$, $\{b_m\}$ and $\{c_m\}$, for $m = [1, M]$ and the independent variable ‘n’.

$$\hat{E}(n|\psi) = \sum_{m=1}^M G_m(n) = \sum_{m=1}^M A_m e^{-0.5 * \left(\frac{n-b_m}{c_m}\right)^2} \quad (4)$$

Here ψ is vector containing the set of model parameters $\{A_m\}$, $\{b_m\}$ and $\{c_m\}$. A curve based on this model function is fitted onto $E(n)$ using Levenberg–Marquardt (LM) optimization scheme by iteratively updating ψ . The fit accuracy is measured by the residuals $\Delta(n)$, in (5), and the best-fit curve is the one that minimizes ‘S’, the sum of squared residuals, in (6).

$$\Delta(n) = E(n) - \hat{E}(n|\psi). \quad (5)$$

$$\text{and } S = \sum_n \Delta(n) \quad (6)$$

The number of Gaussians, M , is adaptively decided in the initial stage, based on identifying the number of prominent peaks in $E(n)$ employing a thresholding scheme. Further, approximate model parameter values are given to the LM optimization block as the initial guess. Initial guesses for $\{A_m\}$ and $\{b_m\}$ are, respectively, the amplitudes and locations of the prominent peaks of $E(n)$. Further, the initial guess for $\{c_m\}$ is assigned as 0.23 times the full width tenth maximum (FWTM). For any ultrasound transducer, its center frequency dictates the value of spatial pulse length and, therefore, the value of FWTM.

Once the model parameters are estimated by the alluded curve fitting method, $E(n)$ is decomposed to M individual Gaussians (G_m). Since in the ROI, the wall layer echoes possess the strongest intensity, the two Gaussians G_I and G_A

with the highest amplitudes A_I and A_A , are identified. These correspond to the intima and adventitia echoes, respectively. The $(b_m - 2 \cdot c_m)$ locations of these Gaussians are evaluated as their leading edges. Therefore, the desired interfaces are evaluated as $LI = (b_I - 2 \cdot c_I)$ and $MA = (b_A - 2 \cdot c_A)$. The wall thickness surrogate is evaluated as,

$$sIMT = \left(\frac{c}{2f_s} \right) \cdot (LI - MA), \quad (7)$$

where c is the speed of the sound propagation in tissue ($=1540$ m/s) and f_s is the sampling frequency of the radiofrequency signal.

D. Simulation Assessment of Method's Robustness

The functionality and robustness of the proposed method were initially assessed on simulated A-mode frames in a systematic manner by the addition of white noise. A simulation testbed was generated that allowed configuring the locations of individual RF echoes (both static and dynamic). This was achieved by first generating a tissue scattering function $TSF(n)$ that consisted of an impulse train with each impulse at user-designated locations $\{k\}$, as expressed in (8). The impulses were further weighted to denote the echogenicity of a particular simulated tissue structure. The so generated $TSF(n)$ when cross-correlated with a unity amplitude Gaussian modulated sinusoidal wavelet $G(n)$ and added with white noise $w(n)$ resulted in the A-mode frame $r(n)$ as shown,

$$TSF(n) = \begin{cases} A_k \delta_k(n), & \text{if } n = k \\ 0, & \text{otherwise} \end{cases} \quad (8)$$

$$\text{and } r(n) = TSF(n) * G(n) + w(n). \quad (9)$$

Here, δ_k and A_k are the impulse at location k and its amplitude, respectively. The signal-to-noise ratio of $r(n)$ is controlled by the amplitude of $w(n)$ and is defined as the

$$SNR = \frac{\text{Amplitude of largest wall echo}}{\text{Amplitude of noise added}}. \quad (10)$$

The objectives of the simulation study are as follows,

- To investigate the performance of the proposed method over a wide range of frame SNR (0 to 40 dB).
- To define the range of SNR for which accuracies are acceptable.

E. Phantom Evaluation of Measurement Feasibility

The proposed method was incorporated to the computing software of our established image-free ultrasound technology, ARTSENS[®]. The measurement feasibility was assessed on a pulsatile flow-phantom setup (Fig. 2). The setup consisted of an elastic carotid mimicking phantom (CNB-STXV, Shelly Medical Imaging Technologies, Canada), connected in a closed flow loop via a physiological pump (CompuFlow1000 physiological flow pump, Shelly Medical Imaging Technologies, Canada) that generates a pulsatile flow of an ultrasound compatible blood-mimicking fluid. A pre-programmed flow waveform was selected from the pump's software interface, and the flow settings were adjusted to vary the minimum and pulse pressure inside the carotid phantom. Based on the pressure inside the phantom,

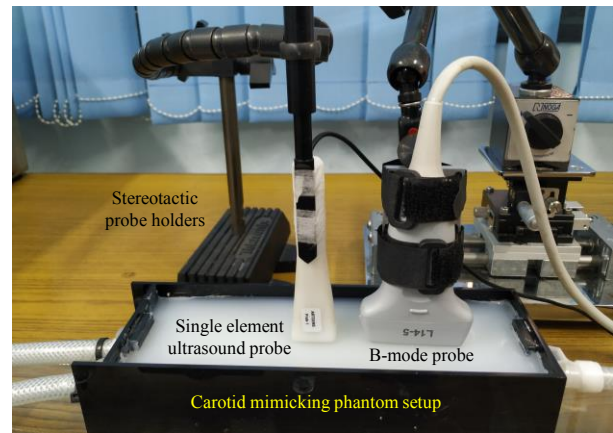


Figure 2. Phantom experimental setup with simultaneous recording by the image-free ARTSENS[®] device and B-mode imaging system.

the wall thickness varied with each setting. The phantom allowed stable beat-to-beat pulsatile flow conditions, therefore, provided a controlled environment to assess the method's performance.

The phantom's mean wall thickness measurements were simultaneously performed by our ARTSENS[®] Pen device with the newly incorporated method and a reference B-mode imaging system (Ultrasonix SonixTouch Q+, BK Medical[®], United States). Imaging data from the B-mode system was acquired as video graphic cine-loops and was post analyzed manually for the wall thickness (WT) measurements. During the calculation of wall thickness, acoustic velocities within the phantom material were appropriately accounted for (carotid-model wall = 1020 m/s, blood mimicking fluid = 1548 m/s). The primary objectives of the phantom study were

- To investigate the measurement feasibility on a phantom setup.
- To evaluate the measurement repeatability (beat-to-beat) and accuracy in a controlled manner.

F. Statistical Analysis

Root-mean-square-error (RMSE) was evaluated to quantify the measurement accuracy during simulations. The average values are represented as mean \pm standard deviation. In the phantom experiments, the comparison between the proposed method's measurements and reference imaging system measurements was made employing linear regression and Bland-Altman (BA) analyses. The strength of agreement is represented by correlation coefficient 'r' along with the statistical significance of the correlation. The significance of mean bias from the BA analysis was evaluated using paired t-test (two samples for mean) with a significance level 0.05. Also, the accuracies were reported as average absolute error percentage. The variability in the beat-to-beat measurements was quantified as the ratio of standard deviation to mean (in %), as an index of repeatability.

III. RESULTS AND DISCUSSION

For frames with 30 dB and 5 dB SNR, the simulated reference IMT (in black line) versus the measured sIMT (green bullet markers) waveforms are shown in Fig. 3(a) and 3(b), respectively. The RMSE between the reference IMT and tracked sIMT for the simulated SNR range is illustrated

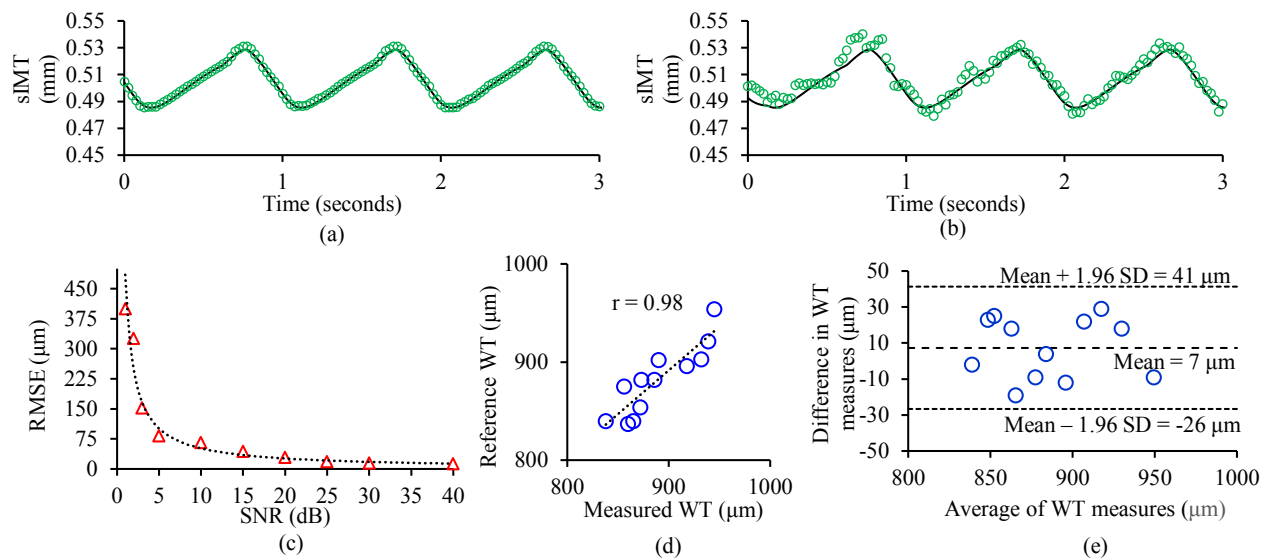


Figure 3. (a) and (b) Simulation versus estimated sIMT for the simulated frames with SNR 30 dB and 5 dB, respectively. (c) RMSE obtained for various SNR frames simulated. (d) Linear Regression plot indicating the correlation between the image-free and imaged based wall thickness measurements from phantom and (e) Corresponding Bland-Altman analysis

in Fig. 3(c). These results indicate the ability of the proposed method to track continuous wall thickness waveforms, with $RMSE < 30 \mu m$ for $SNR > 20 \text{ dB}$. Typically, the expected SNR of A-mode frames from human subjects is greater than 20 dB for which the method exhibited appreciable accuracy during simulations. The performance of the method for the moderate SNRs (5 to 15 dB) is also acceptable with $RMSE < 80 \mu m$.

During the phantom study, high fidelity A-mode frames with $SNR > 25 \text{ dB}$ were recorded, ensuring reliable evaluation of WT. The plots for linear regression and BA analyses for the phantom study are shown in Fig. 3(d) and 3(e), respectively. A strong and statistically significant correlation was observed between the measured versus reference values ($r = 0.88$ and $p < 0.05$). Further, the BA analysis demonstrated a mean bias of $7 \mu m$ that was statistically insignificant ($p = 0.16$) and revealed that measurements are in agreement with each other within the limits of ($-26 \mu m, 41 \mu m$). An absolute percentage error of $(2 \pm 1) \%$ and RMSE of $19 \mu m$, in addition to the above statistical comparisons, demonstrated the method's accuracy performance. The phantom study also demonstrated the beat-to-beat measurement repeatability of the method, with a variability smaller than 2.5%.

In conclusion, the presented method demonstrated its potential for evaluating the surrogate wall thickness in a continuous fashion and in real-time from A-mode frames, as evidenced in light of the simulation and phantom study results. While the results reveal the method's appreciable performance, in-vivo studies on human subjects are warranted to fully validate the same. Our efforts in this regard are underway, where clinical validation studies are being conducted.

REFERENCES

- [1] P. M. Nilsson, P. Boutouyrie, and S. Laurent, "Vascular aging: A tale of EVA and ADAM in cardiovascular risk assessment and prevention," *Hypertension*, vol. 54, no. 1, pp. 3–10, 2009, doi: 10.1161/HYPERTENSIONAHA.109.129114.
- [2] M. W. Lorenz, H. S. Markus, M. L. Bots, M. Rosvall, and M. Sitzer,

- "Prediction of clinical cardiovascular events with carotid intima-media thickness: a systematic review and meta-analysis," *Circulation*, vol. 115, no. 4, pp. 459–467, 2007, doi: 10.1161/CIRCULATIONAHA.106.628875.
- [3] M. L. Eigenbrodt *et al.*, "Common carotid artery wall thickness and external diameter as predictors of prevalent and incident cardiac events in a large population study," *Cardiovasc. Ultrasound*, vol. 5, no. 11, pp. 1–11, 2007, doi: 10.1186/1476-7120-5-11.
- [4] P. M. Nabeel, V. K. Raj, J. Joseph, V. V. Abhidev, and M. Sivaprakasam, "Local pulse wave velocity: theory, methods, advancements, and clinical applications," *IEEE Rev. Biomed. Eng.*, vol. 13, pp. 74–112, 2020, doi: 10.1109/RBME.2019.2931587.
- [5] L. M. Van Bortel *et al.*, "Expert consensus document on the measurement of aortic stiffness in daily practice using carotid-femoral pulse wave velocity," *J. Hypertens.*, vol. 30, no. 3, pp. 445–448, 2012.
- [6] A. Avolio, "Arterial stiffness," *Pulse*, vol. 1, no. 1, pp. 14–28, 2013, doi: 10.1007/s11906-004-0047-z.
- [7] F. Molinari, G. Zeng, and J. S. Suri, "A state of the art review on intima-media thickness (IMT) measurement and wall segmentation techniques for carotid ultrasound," *Comput. Methods Programs Biomed.*, vol. 100, no. 3, pp. 201–221, 2010, doi: 10.1016/j.cmpb.2010.04.007.
- [8] J. Joseph, P. M. Nabeel, S. R. Rao, R. Venkatachalam, M. I. Shah, and P. Kaur, "Assessment of Carotid Arterial Stiffness in Community Settings with ARTSENS®," *IEEE J. Transl. Eng. Heal. Med.*, vol. 9, pp. 1–11, 2021, doi: 10.1109/JTEHM.2020.3042386.
- [9] J. Joseph *et al.*, "ARTSENS® Pen — portable easy-to-use device for carotid stiffness measurement: technology validation and clinical-utility assessment," *Biomed. Phys. Eng. Express*, vol. 6, no. 2, pp. 1–12, 2020.
- [10] J. Joseph, R. Radhakrishnan, S. Kusmakar, A. S. Thrivikraman, and M. Sivaprakasam, "Technical validation of ARTSENS—an image free device for evaluation of vascular stiffness," *IEEE J. Transl. Eng. Heal. Med.*, vol. 3, no. April, p. 1900213, 2015, doi: 10.1109/JTEHM.2015.2431471.
- [11] J. Wikstrand, "Methodological considerations of ultrasound measurement of carotid artery intima-media thickness and lumen diameter," *Clin. Physiol. Funct. Imaging*, vol. 27, no. 6, pp. 341–345, 2007, doi: 10.1111/j.1475-097X.2007.00757.x.
- [12] R. Demirli and J. Saniie, "Model-based estimation of ultrasonic echoes. Part I: Analysis and algorithms," *IEEE Trans. Ultrason. Ferroelectr. Freq. Control*, vol. 48, no. 3, pp. 787–802, 2001, doi: 10.1109/58.920713.